

Automated Pneumoconiosis Detection on Chest X-Rays Using Cascaded Learning with Real and Synthetic Radiographs

Dadong Wang
Quantitative Imaging, Data61
CSIRO
Sydney, Australia
dadong.wang@csiro.au

Yulia Arzhaeva
Quantitative Imaging, Data61
CSIRO
Sydney, Australia
Yulia.Arzhaeva@csiro.au

Liton Devnath
Electrical Engineering & Computing
University of Newcastle
Newcastle, Australia
Liton.Devnath@uon.edu.au

Maoying Qiao
Quantitative Imaging, Data61
CSIRO
Sydney, Australia
Maoying.Qiao@csiro.au

Saeed Amirgholipour
Quantitative Imaging, Data61
CSIRO
Sydney, Australia
Saeed.Amirgholipourkasmani@csiro.au

Qiyu Liao
Quantitative Imaging, Data61
CSIRO
Sydney, Australia
Qiyu.Liao@csiro.au

Rhiannon McBean
Wesley Medical Imaging
The Wesley Hospital
Brisbane, Australia
Rhiannon.McBean@i-med.com.au

James Hillhouse
Medical Imaging
St Vincent's Hospital
Sydney, Australia
jhil2876@uni.sydney.edu.au

Suhuai Luo
Electrical Engineering & Computing
University of Newcastle
Newcastle, Australia
suhuai.luo@newcastle.edu.au

David Meredith
Coal Services Health
Coal Services
Singleton, Australia
David.Meredith@coalservices.com.au

Katrina Newbigin
Wesley Medical Imaging
The Wesley Hospital
Brisbane, Australia
krnewbigin@gmail.com

Deborah Yates
Thoracic Medicine
St Vincent's Hospital
Sydney, Australia
deborahy88@hotmail.com

Abstract—Pneumoconiosis is an incurable respiratory disease caused by long-term inhalation of respirable dust. Due to small pneumoconiosis incidence and restrictions on sharing of patient data, the number of available pneumoconiosis X-rays is insufficient, which introduces significant challenges for training deep learning models. In this paper, we use both real and synthetic pneumoconiosis radiographs to train a cascaded machine learning framework for the automated detection of pneumoconiosis, including a machine learning based pixel classifier for lung field segmentation, and Cycle-Consistent Adversarial Networks (CycleGAN) for generating abundant lung field images for training, and a Convolutional Neural Network (CNN) based image classifier. Experiments are conducted to compare the classification results from several state-of-the-art machine learning models and ours. Our proposed model outperforms the others and achieves an overall classification accuracy of 90.24%, a specificity of 88.46% and an excellent sensitivity of 93.33% for detecting pneumoconiosis.

Keywords—pneumoconiosis, deep learning, computer-aided diagnosis, black lung

I. INTRODUCTION

Pneumoconiosis is an incurable respiratory illness caused by long-term inhalation of respirable dust. About 25,000 people died of pneumoconiosis globally in 2013 [1]. It is reported that pneumoconiosis kills about 6,000 coal workers in China each year [2]; and in the US, it caused 69,377 deaths during 1970-2004 [3]. In Queensland, Australia, about 165 cases of mine dust lung diseases have been diagnosed since 1984 [4]. With the recent re-emergence of pneumoconiosis [5], more cases are feared to have been missed [6]. Poor dust

control and patchy medical screening are to blame for the resurgence of this potentially deadly disease in developed countries [5, 6].

For pneumoconiosis screening, chest radiographs are acceptable, widely available and relatively inexpensive. The current practice in Australia is that coal miners are required to undergo pre-employment chest X-rays, followed by routine X-ray screenings during the employment, and each X-ray requires two B-readers to review. B-readers are trained to use the International Labour Organization (ILO) Classification protocol [7]. However, the insensitivity of chest radiographs for detection of early or moderate pneumoconiosis limits their efficacy in screening. This also leads to low sensitivity and specificity of chest X-rays when read by a radiologist who is qualified as a B-reader, especially for the detection of pneumoconiosis at an early stage of the disease. Inter- and intra-reader variability in chest radiography has been acknowledged ever since chest radiography was first used to identify and classify pneumoconiosis. Another limiting factor is that there are only 102 B-readers outside the United States [8]. This indicates that B-readers are in very short supply, and in some cases, a large backlog of X-rays could occur. To date, there has been a lack of systematic, automated, and objective systems for detecting the presence and assessing the progression of pneumoconiosis for individual coal miners other than by expert radiologists.

In this paper, we present our latest research results from a project to address the above problems by developing Computer-Aided Diagnosis (CAD) tools for automated pneumoconiosis detection using chest X-rays. In collaboration

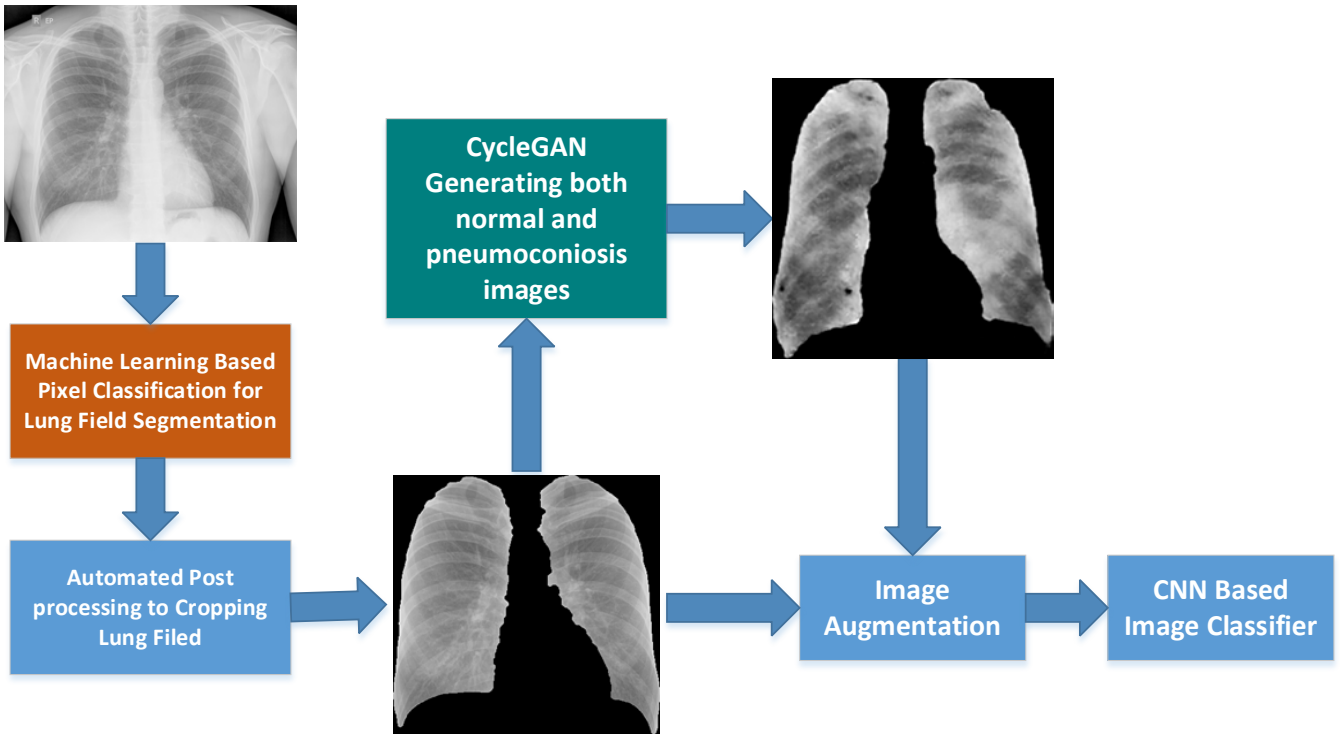


Fig. 1. The overall architecture of the proposed cascade learning model

with Coal Services Health (CSH), St Vincent’s Hospital at Sydney, and Wesley Medical Imaging at Queensland, we developed cascaded machine learning algorithms for the automated pneumoconiosis detection. The rest of the paper is organised as follows: In Section II, we discuss the related works and the challenges in developing deep learning models for automated pneumoconiosis detection. In Section III, we introduce our methods applied to the automated pneumoconiosis detection. In Section IV, we present our experimental results conducted on X-rays captured from coal miners. This is followed by conclusions and future work in Section V.

II. RELATED WORK

Past methods for automated detection of pneumoconiosis include using classical image analysis to extract a set of handcrafted features from each lung field and zone. The features were extracted using based pixel intensities, co-occurrence matrix and frequency domain. A subset of these features were selected as input to train Support Vector Machine (SVM) classifiers to predict whether or not a region of interest in an X-ray contained any abnormalities [9]. This requires substantial work to extract and select the handcrafted features to build the SVM. In the last five years, there have been lots of successful applications of the deep learning methods in medical imaging domain, such as CheXNet [10] for the detection of pneumonia from chest X-rays. The core of CheXNet is a 121-layer dense convolutional neural network (DenseNet) [11] that uses a chest X-ray image as input and generates the probability of pneumonia along with a heat map localizing the areas of the image most indicative of pneumonia. The CheXNet was trained on ChestX-ray14 image database [12] with over 100,000 X-ray images of 14 different thoracic diseases acquired from 30,805 unique patients. When training CheXNet, all pneumonia X-ray images from this database were labelled as positives and

the rest of the images were deemed as negatives. Apart from the large training dataset, 420 chest X-rays were used for testing. The testing results showed that the CheXNet outperformed the average radiologist on pneumonia detection. Pasa et al. proposed a simple convolutional neural network optimised for fast tuberculosis screening using chest X-rays [13]. Unlike most deep learning networks applied to tuberculosis diagnosis, their network is faster and more efficient than previous models but preserves their accuracy. To provide better insight in different deep learning models for X-ray image analysis, ResNets with multiple depths were investigated using transfer learning with and without fine-tuning as well as the training of the ResNets from scratch [14]. The best overall results were reported for the model exclusively trained with Chest X-rays incorporating non-image data such as view position, patient age and gender. Bassi et al. presented a deep convolutional neural network-based classifier for COVID-19 detection using chest X-rays. The classifier is based on DenseNet and can be used to classify an X-ray into one of the three classes: COVID-19, viral pneumonia and normal. The deep CNN was pretrained on ImageNet and then trained on ChestX-ray14 dataset before it was trained on COVID-19 X-rays [15]. Experimental results show that deep learning-based Chest X-ray analysis can be a cheap and accurate auxiliary method for COVID-19 diagnosis. Ozturk et al. presented a model using DarkNet as a classifier for the YOLO object detection system and applied the model to the detection of COVID-19. Their experiments show a classification accuracy of 98.08% for binary classes and 87.02% for multi-class cases [16].

The above studies are based on abundant training samples. However, due to the small incidence of some diseases such as the pneumoconiosis and the restrictions on sharing of patient data, the number of available images may not be sufficient, which leads to imbalanced datasets and introduces significant challenges for training deep learning models. Therefore,

detecting pneumoconiosis on chest X-rays remains a challenging task that relies on the availability of expert radiologists.

In this study, we address the above problems by developing a cascaded machine learning (ML) framework for automated pneumoconiosis detection using both real chest X-rays and synthetic radiographs generated by CycleGAN [17]. To improve the sensitivity and specificity, lung fields are segmented from real chest X-rays using pixel classification and then used to generate synthetic lungs. We also evaluate several popular machine learning models for comparison with our model, including Autoencoder [18] + SVM, Multi-Layer Perceptron (MLP) Learning using KAZE Features [19], and transfer learning based on CheXNet. Experimental results show that our proposed model outperforms others and we achieve overall classification accuracy of 90.24%, a specificity of 88.46% and a sensitivity of 93.33% for detecting pneumoconiosis.

III. METHODS

Deep learning has become very popular and has been used practically in many industry domains. However, one common barrier for deep learning to solve real-world problems remains the amount of labelled training data. In practice, imbalanced datasets often come up with majority of training data from a single class and limited number of training samples from another class. This can lead to biased prediction in favor of the majority class. For the pneumoconiosis detection, we have abundant training data for normal X-rays, however, the number of X-rays with signs of pneumoconiosis is limited. To address this issue, we propose a cascaded learning architecture for the automated pneumoconiosis detection. Fig. 1 shows the architecture which is further detailed in the following sections.

A. Lung Field Segmentation

Lung field segmentation is a pre-requisite for most computer-aided evaluation systems for chest radiographs. We used a pixel-based machine learning algorithm that employs Pixel Classification (PC) to distinguish between lung and non-lung areas in a radiograph [20, 21]. PC yielded around 95% overlap score with the Japanese Society of Radiological Technology (JSRT) gold standard lung masks [22]. We made some necessary modifications to the algorithm to improve its performance so that it worked on both digital and digitized radiographs.

In the training stage an image is resized to a working resolution and subsampled. For each sample in a subsampled image a set of features are extracted. The features are computed from a neighbourhood centred on this sample, and are devised to characterize local image structures using the output of Gaussian derivative filters at multiple scales. In addition, X and Y coordinates of each sample are included in the feature set. Each such feature set has a corresponding label, 0 – if a pixel belongs to image background, 1 – for a pixel in the right lung, and 2 – for a pixel in the left lung. Next, a K -Nearest Neighbour (k -NN) classifier is trained with the feature sets and the corresponding class labels. In the end of the training stage a classifier can compute a probability that a new input pixel belongs to either image background, right lung or left lung.

In the testing stage, a new unknown image is resized to the working resolution, then, the same feature set is computed for

each pixel in the image. A trained k -NN classifier takes each pixel's feature set as an input and computes a probability for that pixel to belong to each of the three classes, p_0 , p_1 and p_2 . This allows us to create a lung probability map P . It has the same size as the test image, and its pixel values, $p(x, y)$, define a probability that a pixel belongs to one of the lung fields:

$$p(x, y) = p_1(x, y) + p_2(x, y) \quad (1)$$

The probability map can be turned into a lung mask by thresholding it at a probability of 0.5, meaning that every pixel that received a probability greater than 0.5 is assumed to be a lung pixel. The two largest connected objects in the resulting binary mask are labelled as 1 (the right lung) and 2 (the left lung), and holes in the masks are filled. To prepare the image data suitable to feed into our CNN image classifier, a post processing function is employed to automatically exclude the black area outside the lung fields. Fig. 2 shows a chest X-ray, its segmented lung fields and automatically cropped lung field images.



Fig. 2. A chest X-ray with parenchymal opacities of pneumoconiosis (left), its lung fields generated by the Pixel Classification (middle) and its cropped lung field image (right).

B. CycleGAN Image Generator

CycleGAN was proposed to capture special characteristics of one image collection and translate the characteristics into the other image collection [17]. It can be used to do image-to-image translation and leverage the imbalanced training datasets. In this work, we train a CycleGAN using selected representative images, including 56 normal and 56 pneumoconiosis lung fields to generate 1,000 normal and pneumoconiosis lung field images, respectively, which include multiple synthetic images generated from a single real X-ray image. Experiments show that overall good accuracy is achieved when using the synthetic images generated by CycleGAN trained for 30 epochs.



Fig. 3. An original lung field X-ray image (left) and a CycleGAN generated X-ray image (right)

C. CNN Based Image Classifier

The input of our CNN based image classifier are images of 256 x 256 in dimension. The classifier is trained to classify an image into the category of either normal or pneumoconiosis.

The CNN model shown in Fig. 1 is composed of 15 neural network layers. It includes 8 convolutional layers to extract feature maps. We start with 32 filters to extract low-level

features, and double the number of filters to 64, then 128 and 256 to detect high-level detailed features. The kernel size used for these filters is 3×3 and stride is 1×1 . The activation function used is ReLU. Four pooling layers are employed to down-sample the feature maps and provide spatial variance. There are also three dense layers, where every input node of each dense layer is connected with every node of its next layer. To avoid overfitting on the proposed model, two dropout layers are used - one between the first and second dense layers, and the other one between the second and third dense layers. The last layer of the classifier uses sigmoid activation function and outputs probability scores for each of the two classes – Normal and Pneumoconiosis.

For the classifier, its input is a chest X-ray downsized to 256×256 pixels, and the output is a binary label $y \in \{0, 1\}$ representing the absence or presence of pneumoconiosis, respectively. During the training, we use binary cross-entropy as a loss function, and RMSprop optimizer. We optimize the binary cross entropy loss:

$$L(\hat{y}, y) = -\frac{1}{N} \sum_{i=1}^N [y_i \log(\hat{y}_i) + (1 - y_i) \log(1 - \hat{y}_i)] \quad (2)$$

where $L(\hat{y}, y)$ is the binary cross loss, y_i is the true value (0 or 1) and \hat{y}_i is the predicted probability of the label y_i , and N is the number of training samples.

D. Image Augmentation

All images including training, validation and testing samples are normalized so that their pixel values are between 0 and 1. For the training images, their mean is set to 0 by subtracting the mean value of the training dataset from each training image. Each training image is also divided by the standard deviation of the training dataset. To increase the diversity of the training dataset, the training images are randomly zoomed with a range of 0.9 to 1.1, and flipped horizontally, and their pixel intensities are sheared with an angle of 0.01 degrees. Apart from scaling the intensities to the range of $[0, 1]$, no other augmentation was done for the validation and testing images.

IV. EXPERIMENTS

In this section, we present our experimental results from the proposed model and compare the results from various popular machine learning models evaluated.

A. Datasets

We collaborated with various organizations to collect image datasets and associated diagnostic labels used in this study. We also use publicly available teaching chest X-ray dataset downloaded from The National Institute for Occupational Safety and Health (NIOSH) website [23] and ILO Standard Radiographs to develop parts of the system. All radiographs used in this study are posterior-anterior (PA) radiographs, some of which are fully digital, while some are digitized films. All X-ray images were captured from mine workers.

Among the image datasets we collected, there are an abundance of normal X-rays, however, only 71 pneumoconiosis images. We set aside 56 pneumoconiosis images (80%) for training and 15 images (20%) for testing. To have balanced classes, we set aside 56 normal images for training and 26 for testing from ILO, NIOSH and Wesley Medical Imaging datasets. The 502 normal images from Coal

Services Health are used for training Autoencoder for feature extraction.

B. Hybrid Model of Autoencoder and SVM

Autoencoders [18] are a specific type of feedforward neural networks where the input is the same as the output. They compress the input into a lower-dimensional code and then reconstruct the output from this code. The Autoencoder can be used as a feature extractor to learn a representation of image data. In this work we used 502 normal X-ray images provided by Coal Services Health to train an Autoencoder for feature extraction. The trained Autoencoder was used to extract features from 56 normal and 56 pneumoconiosis images. The extracted features were employed to train an SVM. The best classification results on the test data are shown in Table I.

C. CheXNet Based Transfer Learning

CheXNet is a deep learning algorithm developed by Stanford Machine Learning Group to detect pneumonia from chest X-rays at a level exceeding practicing radiologists [10]. In this work, we used a pre-trained CheXNet model as a starting point and retrained it using the 1,056 normal and 1,056 pneumoconiosis images, respectively. The 1,056 training images for each class included 1,000 generated by CycleGAN, as explained in Section III.B, and 56 real X-rays. The classification results on the test data are demonstrated in Table I.

D. Multi-Layer Perceptron (MLP) Learning Using KAZE Features

To compare the performance of the proposed model with traditional machine learning approach using handcrafted features, we used KAZE algorithm [19] to extract local features for training a MLP model. The algorithm is a novel multiscale 2D feature detection and description method in nonlinear scale spaces by means of nonlinear diffusion filtering. The evaluation in the paper shows the KAZE outperforms the previous state-of-the-art methods in feature detection and description. Because the number of descriptors for different images varies, we turn the descriptors into a single histogram of visual words using the Bag of Words strategy [24]. The histogram is then used as the input to our MLP neural network.

E. The Proposed Cascaded Learning Framework

To evaluate our proposed model, we used the same training and test datasets as used for retraining the pre-trained CheXNet above. The test dataset includes 41 images (26 normal and 15 pneumoconiosis images), and the training dataset has 1,056 normal and 1,056 pneumoconiosis images, including 1,000 images generated by CycleGAN and 56 real X-rays for each class. For each class, we split the 1,056 images into two datasets with 792 for training (75%), and 264 for validation.

1) *Training of the Image Classifier*: For the training, we used the following hyper parameters: Learning Rate = 0.0001, Epochs = 20, Batch Size = 32. The training was conducted on a GPU workstation with an Intel 18-Core i9 2.6 GHz CPU, 128GB RAM, and 4 Titan Xp GPUs. The training for 20 epochs took only 6 minutes 52 seconds. During the training, the log-loss for the training images was between 0.058 and 0.691, and 0.058 at the end of the training; for the validation images it was between 0.029 and 0.691, and 0.052 at the end of the training. The classification accuracy for the training data

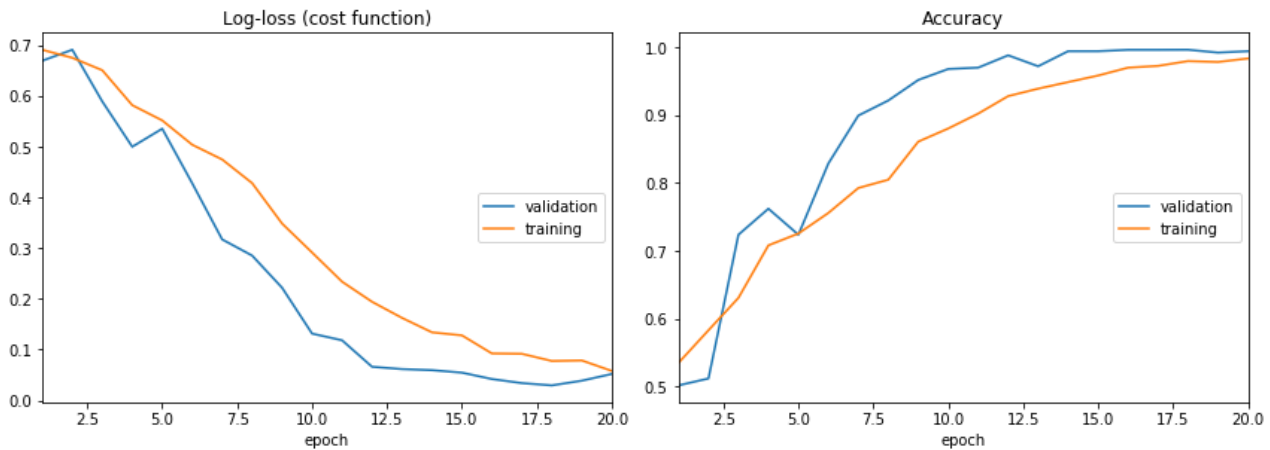


Fig. 4. Loss (left) and accuracy (right) during training and validation

was between 53.5% and 98.3%, and 98.3% at the end of the training; for the validation data it was between 50.2% and 99.6%, and 99.4% at the end of the training. The following figure shows the log-loss and accuracy during the training.

2) *Testing of the Image Classifier:* Only one out of 15 pneumoconiosis X-ray images was misclassified and only 3 out of 26 normal X-rays were misclassified. The overall classification accuracy is 90.24%, the sensitivity is 93.33% and the specificity is 88.46%.

F. Comparison of the Classification Results

The table below compares the results produced by our model and other machine learning algorithms. It clearly shows the proposed model outperforms the others.

TABLE I. COMPARISON OF PNEUMOCONIOSIS DETECTION RESULTS FROM DIFFERENT ML MODELS

Method	Sensitivity	Specificity	Accuracy
MLP + KAZE	66.67%	75%	71.11%
Autoencoder + SVM	73.33%	73.08%	73.17%
CheXNet Based Transfer Learning	73.33%	80.77%	78.05%
Proposed Cascaded Learning	93.33%	88.46%	90.24%

V. CONCLUSIONS AND FUTURE WORK

Pneumoconiosis is deadly and there is no cure for this disease. Early detection of pneumoconiosis through routine medical screening is critical in preventing complications including death. Until now, there has been a lack of systematic, automated, and objective systems for detecting the presence and assessing the progression of pneumoconiosis for individual coal miners other than by expert radiologists.

We develop a cascaded machine learning framework which automatically detects pneumoconiosis from chest X-rays. The proposed method outperforms others and achieves a sensitivity of 93.33%, a specificity of 88.46% and an overall accuracy of 90.24%. We hope this technology can be used for the pre-screening of pneumoconiosis, and to address the issues of variability in identifying pneumoconiosis, and the shortage of B-readers. The cascaded machine learning framework can potentially be used in other medical imaging applications when training datasets are imbalanced or lack diversity.

Future work will encompass a pilot study where our method can be trialled in a clinical setting alongside human readers.

ACKNOWLEDGMENT

This work was funded in part by Coal Services Health and Safety Trust. We thank radiologist Dr Katrina Newbigin from Wesley Medical Imaging for providing examples of nodular dust related lung disease including cases of coal worker's pneumoconiosis and silicosis from their database at The Wesley Hospital. Thanks are also due to Coal Services Health for providing coal mine worker chest X-rays for this study. The authors declare that there is no conflict of interest.

REFERENCES

- [1] GBD 2013 Mortality and Causes of Death Collaborators: Global, regional, and national age-sex specific all-cause and cause-specific mortality for 240 causes of death, 1990-2013: a systematic analysis for the Global Burden of Disease Study 2013. *Lancet*, 385(9963), 117-171 (2015).
- [2] China Daily, "Miners seek justice for black lung disease", http://www.chinadaily.com.cn/china/2011-02/16/content_12021599.htm, February 16, 2011, last accessed 2020/07/31.
- [3] J. Colinet, J. Rider, "Best Practice for Dust Control in Coal Mining", National Institute for Occupational Safety and Health (NIOSH) Publication No. 2010-110, 2010.
- [4] Queensland Government web page, <https://www.business.qld.gov.au/industries/mining-energy-water/resources/safety-health/mining/accidents-incidents/mine-dust-lung-diseases>, last accessed 2020/07/31.
- [5] Reuters Health News dated 24 August 2018, <https://www.reuters.com/article/us-health-coalminers/resurgence-of-crippling-black-lung-disease-seen-in-u-s-coal-miners-idUSKCN1L82FT>, last accessed 2020/07/31.
- [6] M. Sim, D. Glass, R. Hoy, M. Roberts, B. Thompson, R. Cohen, "Review of Respiratory Component of the Coal Mine Workers' Health Scheme for the Queensland Department of Natural Resources and Mines, Final Report", Monash University, 2016.
- [7] International Labor Office, "Guidelines for the use of the ILO International Classification of radiographs of pneumoconioses", Occupational Safety and Health Series, 22, 2011.
- [8] The National Institute for Occupational Safety and Health (NIOSH) Chest Radiography: https://wwwn.cdc.gov/niosh-rhd/cwhsp/ReaderList.aspx?formid=InternationalExaminees&lastname=&sortkey=country&format=table&btnSubmit_Intl=Submit, last accessed 2020/07/31.
- [9] R. Sundararajan, H. Xu, P. Annangi, X. Tao, X. Sun, and L. Mao, "A multiresolution support vector machine based algorithm for

- pneumoconiosis detection from chest radiographs”, 2010 IEEE International Symposium on Biomedical Imaging, pp. 1317-1320, IEEE, Rotterdam, The Netherlands, 2010.
- [10] P. Rajpurkar, J. Irvin, K. Zhu, B. Yang, H. Mehta, T. Duan, D. Ding, A. Bagul, C. Langlotz, K. Shpanskaya, M. Lungren, and A. Ng, “CheXNet: Radiologist-Level Pneumonia Detection on Chest X-Rays with Deep Learning”, arXiv preprint arXiv:171105225, 2017.
- [11] G. Huang, Z. Liu, L. Maaten, and K. Weinberger, “Densely Connected Convolutional Networks”, IEEE Conference on Computer Vision and Pattern Recognition, pp. 2261-2269, Hawaii, USA, 2017.
- [12] X. Wang, Y. Peng, L. Lu, Z. Lu, M. Bagheri, and M. Summers, “ChestX-ray8: Hospital-scale Chest X-ray Database and Benchmarks on Weakly-Supervised Classification and Localization of Common Thorax Diseases”, IEEE Conference on Computer Vision and Pattern Recognition (CVPR), pp. 3462-3471, Hawaii, USA, 2017.
- [13] F. Pasa, V. Golkov, F. Pfeiffer, et al. “Efficient Deep Network Architectures for Fast Chest X-Ray Tuberculosis Screening and Visualization”, Scientific Reports 9, 6268 (2019). <https://doi.org/10.1038/s41598-019-42557-4>.
- [14] I. M. Baltruschat, H. Nickisch, M. Grass, et al., “Comparison of Deep Learning Approaches for Multi-Label Chest X-Ray Classification”, Scientific Reports 9, 6381 (2019). <https://doi.org/10.1038/s41598-019-42294-8>.
- [15] P. Bassi, R. Attux, “A Deep Convolution Neural Network for COVID-19 Detection using Chest X-rays”, arXiv:2005.01578.
- [16] T. Ozturk, M. Talo, E. A. Yildirim, U. B. Baloglu, O. Yildirim, and U. R. Acharya, “Automated detection of COVID-19 cases using deep neural networks with X-ray images”, Comput Biol Med. 2020 Jun; 121: 103792. doi: 10.1016/j.compbiomed.2020.103792.
- [17] J. Zhu, T. Park, P. Isola, and A. Efros, “Unpaired Image-to-Image Translation using Cycle-Consistent Adversarial Networks”, IEEE International Conference on Computer Vision (ICCV), pp. 2223-2232. IEEE, Venice, Italy, 2017.
- [18] D. Kingma, and M. Welling, “Auto-encoding variational bayes”, arXiv:1312.6114, 2013.
- [19] P. Alcantarilla, A. Bartoli, and A. Davison, “KAZE features”, In: Eur. Conf. on Computer Vision (ECCV), pages 214–227. IEEE, Italy (2012).
- [20] B. Van Ginneken, M. B. Stegmann, M. Loog, “Segmentation of anatomical structures in chest radiographs using supervised methods: a comparative study on a public database”, Medical Image Analysis, 10, 19–40, 2006.
- [21] A. Wan, W. Zaki, and M. Fauzi, “Lung segmentation on standard and mobile chest radiographs using oriented Gaussian derivatives filter”, Biomed Eng Online, 14-20 (2015).
- [22] Japanese Society of Radiological Technology (JSRT) Database: <http://db.jsrt.or.jp/eng.php>, last accessed 2020/07/31.
- [23] The National Institute for Occupational Safety and Health (NIOSH) B Reader Study Syllabus, <https://www.cdc.gov/niosh/topics/chestradiography/breader-study-syllabus.html>, last accessed 2020/07/31.
- [24] F. Li, R. Fergus, A. Torralba, “Recognizing and learning object categories”, CVPR Short Course (2007).